지구물리 | Vol. 9, No. 3, Special Volume, pp. 241-248, 2006 | J Korean Geophysical Soc

Moho Depth Variation and Vp/Vs ratios in the Southern Korean Peninsula from Teleseismic Receiver Functions

H. J. Yoo*,, K. Lee* and R. B. Herrmann*****

*Korea Polar Research Institute, KORDI
Songdo Techono Park, 7-50, Songdo-dong,Yeonsu-gu, Incheon, 406-840, South Korea
**School of Earth and Environmental Sciences
Seoul National University, Seoul 151-742, South Korea
***Department of Earth and Atmospheric Sciences, Saint Louis University
331 North Grand Boulevard St. Louis, MO 63108 U.S.A

ABSTRACT

In this study, we applied the teleseismic receiver function technique to determine the crustal thicknesses and Vp/Vs ratios for 31 broadband stations of the Korean Peninsula and map out the lateral variation of Moho depth in the Peninsula. The estimated depths to Moho range from 26 to 35 km except for an island station ULL (17 km). The Moho is turned out to be deeper in the south-western part of the Peninsula and western Gyeongsang basin, and shallower in the off-shore region close to East Sea (Sea of Japan). The Vp/Vs ratio varies from 1.69 to 1.89 with the average of 1.77, which is close to global average (1.78) in the crust.

Key words

receiver function, Moho, Vp/Vs ratio, the Korean Peninsula

1. Introduction

The crust and underlying mantle are separated by the Mohorovicic discontinuity (Moho), which represents a major change in seismic velocities, chemical compositions, and rheology. The Moho depth and morphology is one of the most important features to characterize the overall structure of the lithosphere, i.e. it is a key to the reconstruction of the tectonic evolution of the region.

In the past decades, the estimation of Moho depth in the Korean Peninsula has been attempted using both seismic (Lee, 1979a; Kim and Kim, 1983; Kim, 1995 Song and Lee, 2001) and gravity data (Lee, 1979b Kwon and Yang, 1985; Choi and Shin 1996; Kim *et al*., 2003). Lee (1979a) first investigated the crustal structure of the Peninsula based on the travel time data of the Ssanggyesa earthquake of July 4, 1936 and proposed a simple one-layered crustal model in which the crust has a thickness of about 35 km and Pn- velocity is about 7.7 km/sec. Subsequent studies of Kim and Kim (1983) and Kim (1995) suggested two- and three-layered crustal model with Moho at the depth of about 32 km. Gravity anomaly studies estimated the Moho depth of the Peninsula to be about 32 km in average (Kwon and Yang, 1985; Choi and Shin 1996; Kim *et al*., 2003) and there is no clear evidence of pronounced discontinuity in the crust (Kwon and Yang, 1985). Most recently, Chang and Baag (2005) and Yoo *et al*. (2006) mapped the crustal thickness variation in the Peninsula by receiver function method. It is a general agreement among these studies that the average crustal thickness in the Peninsula is about 33 km in average with thicker crust in the southern part and thinner crust in middle part of the Peninsula. But there are still some differences in Moho depth beneath several regions.

In this study, we derived the variation of Moho depth and V_P/V_S ratios from the teleseismic data of 31 broadband stations which are rather uniformly distributed in the Peninsula by receiver function stacking method of Zhu and Kanamori (2000). The resultscan be one clue to the crustal evolution of the Korean Peninsula.

2. Data

Digital seismology in Korea began with the installation of the IRIS station at Inchon. Subsequently, the Korean Institute of Geoscience and Mineral Resources (KIGAM)

Corresponding Author : H. J. Yoo (jhyoo@kopri.re.kr)
원고접수일 : 2006년 8월 25일 게재승인일 : 2006년 9월 18일

installed some broadband stations. In 2000, the Korean Meteorological Administration (KMA) digital seismic network became operational. The KMA network has a backbone of broadband stations, some additional short- period stations, and a dense network of accelerometers transmitting continuous data to the analysis center in Seoul. In addition, additional broadband and accelerometers sensors are in operation by the Korea Institute of Nuclear Safety (KINS) and the Korean Electric Power Research Institute (KEPRI).

This study uses P-wave radial receiver functions derived from 31 broadband seismic stations which are uniformly distributed in the Peninsula (Fig. 1). The receiver functions are estimated using the iterative time-domain deconvolution technique of Ligorria and Ammon (1999) from 92 event data. Most of the events are distributed in the south back-azimuth direction (Indonesia through Papua New Guinea to the Fiji) while some in the northeast (Aleutian Trench and Alaska region) and west (India and Iran) back-azimuth direction (Fig. 2). The good epicentral distance and azimuthal coverage helps to average out lateral structural variations.

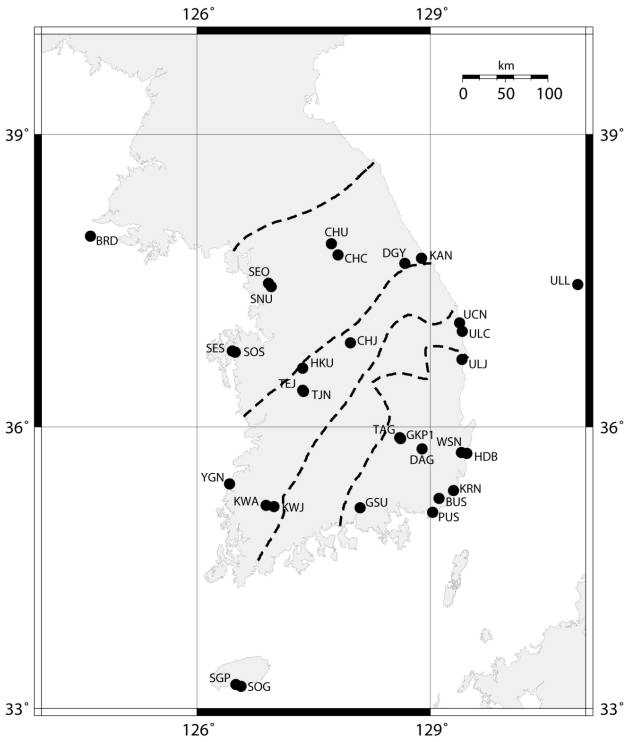

Fig. 1 Locations of the three-component broad-band (STS-1) seismic stations used in this study. Major tectonic boundaries are shown as dashed lines.

3. Method

P to S converted phases and S multiples originating from near receiver velocity discontinuities have been used to estimate Moho depth and Vp/Vs ratios under a seismic station since the pioneering study of Zandt and Ammon (1995). The time delay between the first arriving direct wave and the associated converted phases is a function of the depth and velocity structure of the medium (see Fig. 3). Using the time difference between the Ps phase and the first arrival Pp, the depth to Moho can be estimated from the following equation:

$$H = \frac{t_{Ps}}{\sqrt{\frac{1}{V_S^2} - p^2} - \sqrt{\frac{1}{V_P^2} - p^2}} \qquad (1)$$

where H is the depth to Moho, t_{Ps} is the time delay between the first arrival and the Ps, p is the ray parameter, and V_P and V_S are the velocity of P- and S-wave, respectively. The crustal thickness, however, trades off strongly with the seismic wave velocity since the delay time of the S leg

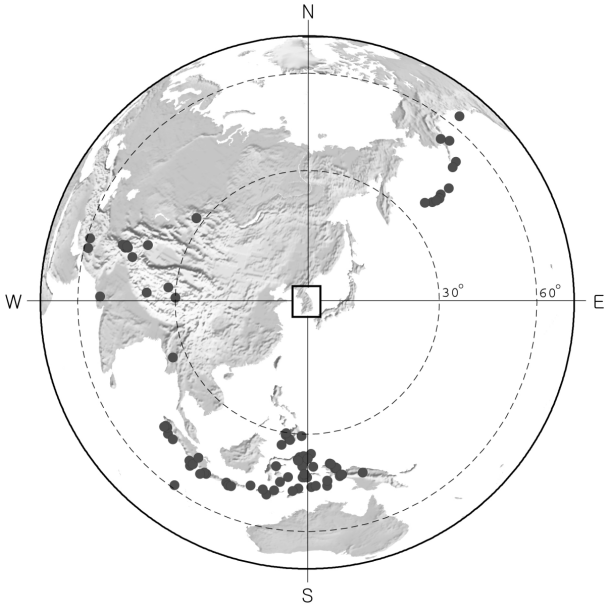

Fig. 2 Epicenter distribution of teleseismic events used in this study. The map center is 128.0°W, 37.0°N. The topography is from ETOPO05.

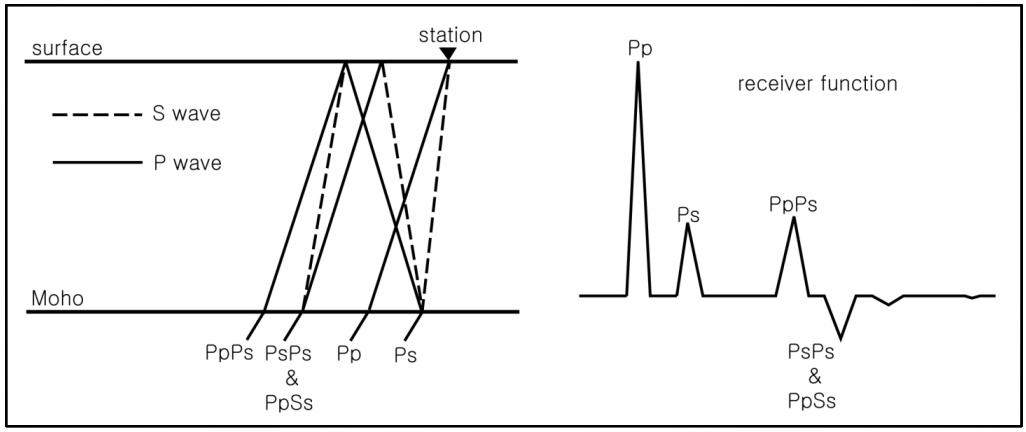

Fig. 3 Cartoon showing direct P (labeled Pp) and the dominant crustal reverberations, where, exceptfor mantle P, lowercase and uppercase indicate up-going and down-going rays, respectively, and the associate receiver function after Ammon *et al*. (1990).

is dependent on the shear velocity of the medium (Zhu and Kanamori, 2000). Incorporating secondary converted phases (PpPs, PpSs, and PsPs in Fig. 3) can help reduce this trade-off significantly. The time delays for secondary multiples and H can be expressed as follows:

$$H = \frac{t_{PpPs}}{\sqrt{\frac{1}{V_s^2} - p^2} + \sqrt{\frac{1}{V_P^2} - p^2}}, \qquad H = \frac{t_{PpSs+PsPs}}{2\sqrt{\frac{1}{V_s^2} - p^2}}, \tag{2}$$

In reality, identifying the Moho Ps and the multiples and measuring their arrival times on a single receiver function trace can be very difficult due to background noise, scatterings from crustal heterogeneities, and P-to-S conversions from other velocity discontinuities. Zhu and Kanamori (2000) developed a slant stacking approach, which essentially transforms the receiver function stacks from the time domain to the $H-k$ domain (we designate V_P/V_S as k), in order to straightforwardly estimate the depth to Moho and V_P/V_S ratios. The great advantage of this method is that there is no need to pick the arrival times of the direct conversion from the Moho and its multiples. The receiver function stacking in the $H-k$ domain is defined by:

$$s(H,k) = w_1 r(t_1) + w_2 r(t_2) - w_3 r(t_3) \tag{3}$$

where $r(t)$ is the radial receiver function, t_1, t_2 and t_3 are the predicted Ps, PpPs, and PpSs+PsPs arrival times corresponding to crustal thickness H and V_P/V_S ratio (k), as given in (1) and (2). The w_i are weighting factors, and $\sum w_i = 1$. The $s(H,k)$ reaches a maximum when all three phases are stacked coherently with the correct H and k.

Uncertainties of H and V_P/V_S can be estimated from the flatness of $s(H,k)$ at the maximum after taking Tayler series expansion for $s(H,k)$ and omitting the higher-order terms, i.e. one can get the variances of H and k by:

$$\sigma_H^2 = 2\sigma_s / \frac{\partial^2 s}{\partial H^2}, \qquad \sigma_k^2 = 2\sigma_s / \frac{\partial^2 s}{\partial k^2} \tag{4}$$

where σ_s is the estimated variance of $s(H,k)$ from stacking.

4. Analysis and Results

We colletted waveforms of 92 teleseismic earthquakes recorded by broadband stations of the Korean Peninsula. The actual number of events for individual station varies from 1 to 35, depending on the length of recording period and background noise level of the station (Table 1). We used a time window of 70s in length, starting 10s before the P onset, to obtain the P waveform from raw velocity records. The iterative time domain deconvolution technique then was applied to get receiver functions from raw data. We chose Gaussian width factor alpha to be 2.5, which

Table 1 Crustal thickness and *Vp*/*Vs* ratio under the broadband stations.

STATION	H(km)	Vp/Vs	Poisson Ratio	Vertical P wave Travel time(RS)	Event #	Comment
BRD	33.7±3.6	1.74±0.15	0.253	5.20±0.56	3	alpha=1.0
BUS	34.3±1.7	1.77	0.266	5.29±0.26	4	fixed Vp/Vs
CHC	30.5	1.77	0.266	4.71	1	fixed Vp/Vs
CHJ	31.8±1.3	1.77	0.266	4.91±0.20	4	fixed Vp/Vs
CHU	31.7±1.2	1.78±0.05	0.269	4.89±0.18	21	
DAG	34.6±1.1	1.79±0.05	0.275	5.34±0.17	4	
DGY	31.8±1.2	1.77	0.266	4.91±0.18	3	fixed Vp/Vs
GKP1	33.8±1.2	1.81±0.05	0.281	5.22±0.18	8	
GSU	31.9±2.7	1.83±0.11	0.289	4.92±0.42	35	alpha =1.0
HDB	28.5±1.6	1.77	0.266	4.40±0.25	14	fixed Vp/Vs
HKU	32.0±2.0	1.77±0.06	0.266	4.94±0.31	16	
KAN	27.5±1.5	1.80±0.06	0.276	4.24±0.23	15	
KRN	31.8±1.8	1.77	0.266	4.91±0.28	19	fixed Vp/Vs
KWA	29.8±2.3	1.77	0.266	4.60±0.35	3	fixed Vp/Vs
KWJ	32.5±3.5	1.88±0.16	0.302	5.02±0.54	20	alpha =1.0
PUS	33.0±1.1	1.75±0.06	0.258	5.09±0.17	15	
SEO	29.9±1.5	1.73±0.06	0.251	4.61±0.23	23	
SES	31.3±1.8	1.77	0.266	4.83±0.28	17	fixed Vp/Vs
SGP	33.6±0.7	1.69±0.04	0.232	5.18±0.11	2	
SNU	30.2±1.3	1.74±0.06	0.253	4.66±0.20	17	
SOG	33.8±1.2	1.74±0.06	0.255	5.22±0.18	5	
SOS	29.0±1.6	1.77	0.266	4.48±0.25	4	fixed Vp/Vs
TAG	34.0±2.4	1.80±0.07	0.278	5.25±0.37	15	
TEJ	33.3±1.2	1.72±0.04	0.246	5.14±0.18	16	
TJN	33.6±0.9	1.71±0.04	0.238	5.19±0.14	18	
UCN	28.3±3.3	1.77	0.266	4.37±0.51	28	fixed Vp/Vs
ULC	25.5±0.6	1.75±0.04	0.259	3.94±0.09	4	
ULJ	28.2±1.4	1.817±0.08	0.283	4.35±0.22	17	
ULL	16.5±1.0	1.77	0.266	2.55±0.15	15	fixed Vp/Vs, Vp=6.2
WSN	27.4±1.3	1.81±0.07	0.279	4.23±0.20	25	
YGN	35.3±1.5	1.77	0.266	5.45±0.23	26	fixed Vp/Vs

corresponds to a cutoff frequency of 1.0 Hz for most of stations. In case $H-k$ grid search does not converge, due to receiver functions without clear multiples or noise at high frequency level, we used alpha=1.0, which corresponds to 0.3 Hz low-pass filter. The receiver functions of each station are then stacked using (3), with $w_1 = 0.7$, $w_2 = 0.2$, $w_3 = 0.1$ according to the suggestions of Zhu and Kanamori (2000). Among phases we used, the Ps has the highest Signal to Noise ratio (SNR) so it is given a higher weight than the other two. All stacking are done using an average crustal P velocity of 6.48 km/s except for 6.2 km/s for ULL station. Crustal thickness and V_P/V_S ratio are obtained from the location of $s(H,k)$ maximum. Their uncertainties are estimated by (4).

As an example, stacking 25 receiver functions for station WSN gives a crustal thickness of 27.4 km with a crustal Vp/Vs ratio of 1.81 (Fig. 4a). The predicted Moho Ps arrival time agrees with the receiver function profile which shows a strong converted phase at 3.3 s following the direct P arrival (Fig. 4b). This phase has the expected increased

of amplitude and time delay with ray parameter for a primary converted phase.

Station GSU, one of stations having good data coverage, has a total of 35 receiver functions. The low frequency (alpha=1.0) receiver functions, however, are used in receiver function stacking because we it is hard to obtain converging $s(H,k)$ with high frequency (alpha=2.5) receiver functions during grid search process (Fig. 5a). Crustal thickness under the station is estimated to be 31.9 km with a crustal Vp/Vs ratio of 1.84 (Fig. 5b).

There are other apparently coherent phases after the Moho Ps in the above receiver function profiles. They might be generated by P-to-S conversions from some upper mantle discontinuities, or the multiples of intracrustal

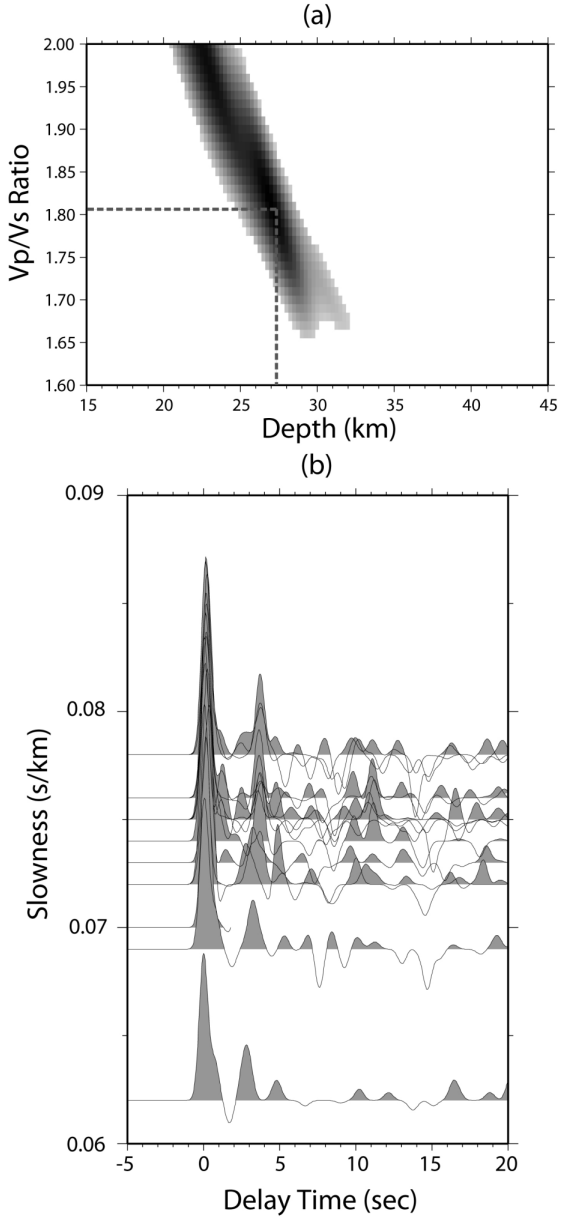

Fig. 4 (a) The $s(H, k)$ for station WSN. The best estimate of the crustal thickness is 27.4 km with Vp/Vs ratio of 1.81. (b) Receiver function (alpha = 2.5) profile used in calculating crustal thickness and Vp/Vs ratio.

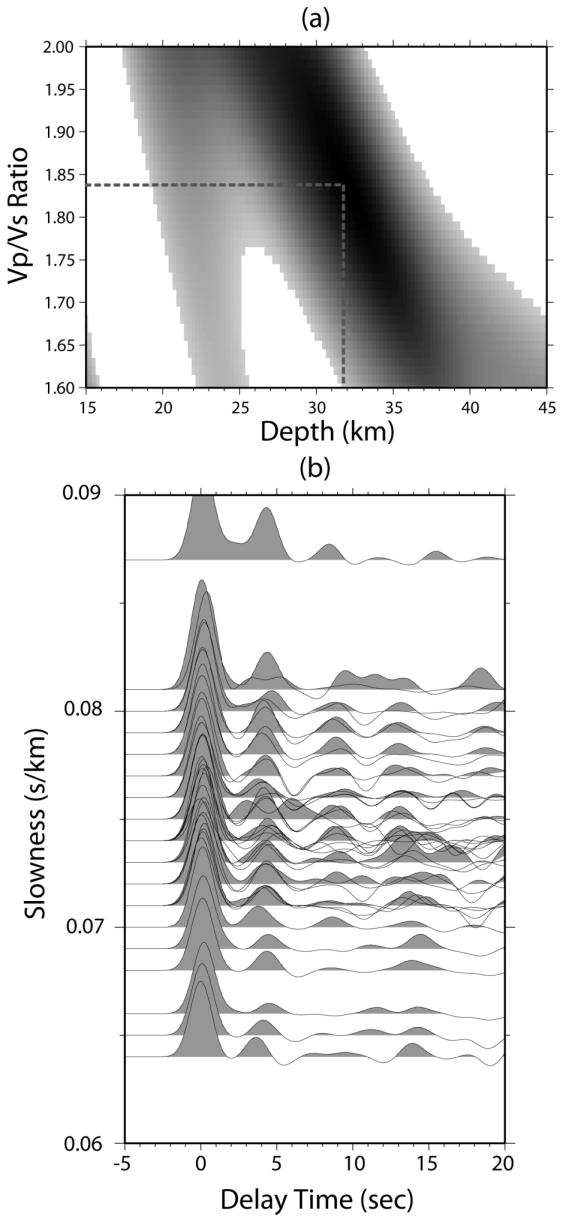

Fig. 5 (a) The $s(H, k)$ for station GSU. The best estimate of the crustal thickness is 31.9 km with Vp/Vs ratio of 1.84. (b) Receiver function (alpha = 1.0) profile used in calculating crustal thickness and Vp/Vs ratio.

conversions. In principle, these phases have different moveouts with ray parameter from those of Moho PpPs and PpSs+PsPs, so their energy will not stacked coherently in $s(H,k)$. However, the presence of these phases often smears the $s(H,k)$ maximum and sometimes causes other local maxima. In the case of multiple peaks in $s(H,k)$, information on the crustal thickness and Vp/Vs ration from nearby stations or other sources can help resolve the ambiguity.

Altogether, we obtained 19 Vp/Vs ratio and 31 crustal thickness measurements from 31 broadband stations. The final thickness and Vp/Vs ratio results are enumerated in Table 1. The crustal Vp/Vs ratio ranges from 1.69 to 1.89 with the average of 1.77. The crustal thickness of southern Korean Peninsula is 31 km in average however, there is a wide range of values from 26 to 35 km except for the island station (17 km of ULL station).

5. Discussion and Implications

Moho depths under each station were combined using minimum curvature technique (Smith and Wessel, 1990) to produce a continuous Moho depth variation of southern Korean Peninsula (Fig. 6). Although the grid spacing is a little bit wide for the interpolation, it can be seen as gross pattern of crustal thickness variation. The Moho is found to be deeper under the south-western part of the Peninsula and western Gyeongsang basin, while shallower Moho exist in the off-shore region faced with East Sea (Sea of Japan). The topography of the Moho in the Gyeonggi massif is relatively flat around the average depth and becomes shallower to the east and deeper to the south. These features are in good agreement with the previous receiver function studies (Chang and Baag 2005, Yoo *et al*., 2006). Yoo *et al*. (2006) reported that the deepest Moho is found in the southwestern part, where is one of the wide mountain regions, of the Peninsula but we could not findany evidence due to lack of data in the region in this study.

A map of the Vp/Vs ratios (Fig. 7) was compiled from the grid search results listed in Table 1. The average value in the Peninsula is 1.77 which is close to the global average in the crust estimated by Zandt and Ammon (1995). Higher Vp/Vs ratios are measured beneath the southern Peninsula (stations DAG, TAG, GKP1, GSU, KWJ) making maximum at KWJ station (1.88). Smaller values (1.71-1.74) are obtained inthe middle part of the Peninsula (stations SEO, SNU, TEJ, TJN), and the lowest value at Cheju

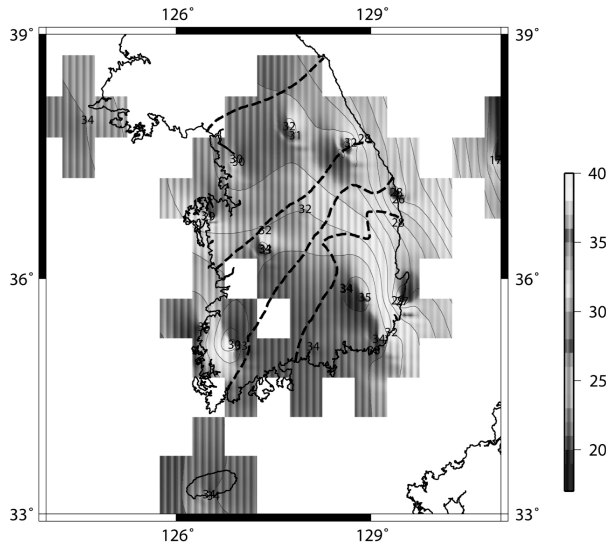

Fig. 6 Distribution of the Moho depths in southern Korean Peninsula estimated by receiver function stacking method. Interpolation is performed using "minimum curvature" technique (Smith and Wessel, 1990). Locations and Moho depths used in the interpolation are shown in the map. Major tectonic boundaries are shown as dashed lines.

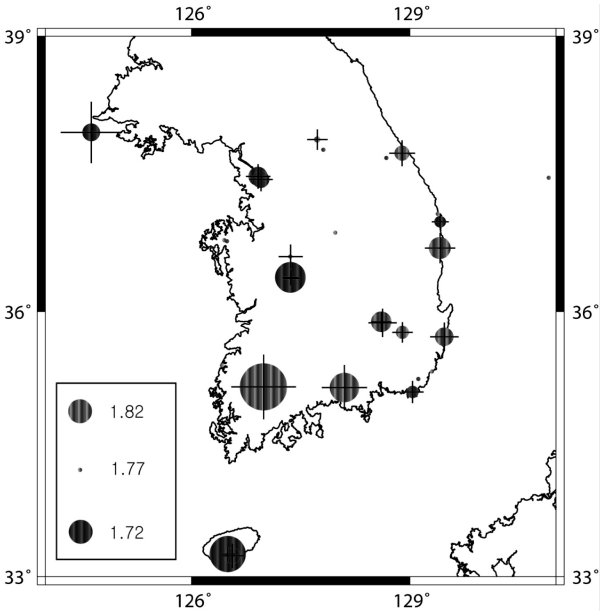

Fig. 7 The estimated crustal Vp/Vs ratios (circles) for 31 broadband stations. Their uncertainties are represented by the sizes of the crosses.

Island (1.69 at SGP).

Unfortunately, crustal Vp/Vs ratio is among the least constrained parameters from both laboratory and field measurements. It is thought that the average composition of the continental crust is close to andesite or diorite (Anderson, 1989). Laboratory measurements of the Vp/Vs ratio of diorite at crustal pressures range from 1.75 to 1.79 (Carmichael, 1982). Christensen (1996) estimated an average Vp/Vs ratio for the continental crust to be about 1.76 from laboratory measurements of typical crustal rocks. Zandt and Ammon (1995) estimated Poisson's ratio of different types of continental crust; the global average is 0.27 which corresponds to Vp/Vs ratio of 1.78. For the Mesozoic and Cenozoic belts they obtained a lower ratio (1.732) with large variations.

There exist several possibilities to explain relatively high values of Vp/Vs ratio. Generally, a sedimentary cover containing layers with very low shear wave velocities may influence the distribution of Vp/Vs ratios. Most of stations in this study are on crystalline rocks except for some stations in the Gyeongsang basin (DAG, TAG, GKP1). Cho *et al*. (2006) found about 3 km thick sedimentary layers with 2.9 to 3.2 km/s of S-wave velocities in the Gyeongsang basin using tomography study of surface-wave. High Vp/Vs ratios at these stations might be influenced by these thick sedimentary layers. Another possibility to explain high values of Vp/Vs is the presence of thick 'basaltic' (Vs around 4.0 km/s) layer in the lower crust. Possibly, the very high value of Vp/Vs at KWJ station is influenced by the anomalously thickened basaltic layer which may be caused by recent magmatic underplating (Yoo *et al*., 2006).

The observed low anomaly in Vp/Vs ratio could be caused by structural effects such as topography at the Moho. Zandt *et al*. (1995) obtained Vp/Vs ratios of 1.62 to 1.64 for the westernmost Basin and Range Province, North America. They suggested the very low values in that region are possibly caused by the breakdown of the assumption that the crust is laterally homogeneous. A lateral change in crustal thickness of 5 km together with an unchanged Ps delay time would lead to a Vp/Vs change of 3.5% (1.67 instead of 1.73) according to Zandt *et al*. (1995). Direct conversions (Ps) and multiples sample different paths within the crust. Therefore, lateral variations also may influence the results. However, since the topography of Moho in the Korean Peninsula does not show such an inhomogeneous feature (Chang and Baag, 2005; Yoo *et al*., 2006), this is not the reason of low Vp/Vs values in the Peninsula.

Another possibility to explain low values is the presence of fluids under normal pore pressure within pores of low aspect ratio or high quartzs content in the crust (Christensen, 1996). We suppose that low value of Vp/Vs at SGP may be caused by quartz-rich rocks or the presence of fluids dominate this region. It could be, otherwise, an artifact due to the uncertainty of the Vp/Vs estimation.

Acknowledgments

This study would not have been possible without the digital data sets provided by the Korea Meteorological Administration (KMA), the Korean Institute for Geosciences and Mineral Resources (KIGAM), and the Korea Institute of Nuclear Safety (KINS). Research at Seoul National University was supported under the BK21 project. Research was supported in part by the Korea Polar Research Institute, KORDI under grant PE06020. Maps were created using GMT (Wessel and Smith, 1995).

References

Anderson, D. L. (1989). Theory of the Earth, Blackwell Sci., Malden, Mass.

Carmichael, R. S (1982) Practical handbook of physical properties of rocks Vol II, CRC Press.

Chang, S. and C. Baag (2005). Crustal Structure in Southern Korea from Joint Analysis of Teleseismic Receiver Functions and Surface-Wave Dispersion, Bull. Seism. Soc. Am., 95, 1516-1534.

Cho,. K. H., R. B. Herrmann, C. J. Ammon, and K. Lee (2006). Imaging the crust of the Korean Peninsula by surface-wave tomography , Bull. Seism. Soc. Am., in review.

Choi,K. S. and Y. H. Shin (1996). Isostasy in and around the Korean Peninsula by analyzing gravity and topography data, J. Geol. Soc. Korea 32, 407-420 (in Korean).

Christensen, N. I. (1996) Poisson's ratio and crustal seismology, J. Geophys. Res., 101, 3139-3156.

Kim, J. W., J. D. Cho, W. K. Kim, K. D. Min, J. H. Hwang, Y. S. Lee, C. H. Park, J. H. Kwon, and J. S. Hwan (2003). Extraction of Moho undulation of the Korean Peninsula from gravity anomalies, Econ. Environ. Geol. 36, 213-223 (in Korean).

Kim,S. J. and S. G. Kim (1983). A study on the crustal structure of South Korea by using seismic waves, J. Korean Inst. Mining Geol. 16, 51-61 (in Korean).

Kim, S. K. (1995). A study on the crustal structure of the Korean peninsula, J. Geol. Soc. Korea 31, 393-403 (in Korean).

Kwon, B. D. and S. Y. Yang (1985). A study on the crustal structure of the southern Korean Peninsula through gravity analysis, J. Korean Inst. Mining Geol. 18, 309-320.

Lee, K. (1979a). On crustal structure of the Koean Peninsula, J. Geol. Soc. Korea 15, 255-258.

Lee, K. (1979b). On Isostasy of the Korean Peninsula, J. Geol. Soc. Korea 15, 134-140.

Ligorria, J. P. and C. J. Ammon (1999). Iterative deconvolution of teleseismic seismograms and receiver function estimation, Bull. Seism. Soc. Am. 89, 1395-1400.

Smith, W. H. F. and P. Wessel (1990). Gridding with continuous curvature splines in tension, Geophysics 55, 293-305.

Song, S. G. and K. Lee (2001). Crustal structure of the Korean Peninsula by travel time inversion of local earthquakes, J. Geophys, Soc. Korea,Vol. 4, 21-33.

Wessel, P. and Smith, W. (1995). New version of the generic mapping tools released. EOS Trans. AGU 76, 329.

Yoo, H. J., R. B. Herrmann, K. H. Cho, and K. Lee (2006). Imaging the Three-Dimensional Crust of the Korean Peninsula by Joint Inversion of Surface-Wave Dispersion and Teleseismic Receiver Functions, Bull. Seism. Soc. Am., in review.

Zandt, G. and C. J. Ammon (1995). Continental-crust composition constrained by measurements of crustal Poissons ratio, Nature, 374, 152-154.

Zandt, G., S. C. Myers, and T. C. Wallace (1995). Crust and mantle structure across the Basin and Range-Colorado Plateau boundary at 37^{o}N latitude and implications for Cenozoic extensional mechanism, J. Geophys. Res., 100, 10529-10548.

Zhu, L. and H. Kanamori (2000). Moho depth variation in southern California from teleseismic receiver functions, J. Geophys. Res., 105, 2969-2980.